Published in final edited form as:
Opt Express. 2009 May 25; 17(11): 8947–8955.

Dual channel dual focus optical coherence tomography for imaging accommodation of the eye

Chuanqing Zhou[1,*], **Jianhua Wang**[2,*], and **Shuliang Jiao**[2,3,**]

[1]Institute for Laser Medicine and Biophotonics, Shanghai Jiao Tong University School of Life Science and Biotechnology, 800 Dongchuan Road, Shanghai 200240, China

[2]Bascom Palmer Eye Institute, University of Miami Miller School of Medicine 1638 NW 10th Ave. Miami, FL 33136, USA

Abstract

A dual channel dual focus spectral-domain optical coherence tomography was developed for imaging the accommodation of the eye in real time. The system can provide simultaneous cross-sectional imaging of all the surfaces of the anterior segment of the eye including the cornea, anterior chamber, anterior and posterior surfaces of the crystalline lens. Thus, the modification of the curvatures of the anterior and posterior surfaces of the crystalline lens and the dimensions of the anterior segment of the eye with accommodation can be calculated. The system was successfully tested in imaging accommodation. The preliminary results demonstrated the feasibility of this novel approach.

1. Introduction

Accommodation is the act of the eye to adjust the refractive power to bring near objects into sharp focus. Accommodation occurs through possible controlled changes in the crystalline lens shape and thickness, and in distances between the major refractive surfaces. The mechanism of accommodation and its relevance to presbyopia has been debated for more than 150 years since the debut of Helmholtz's theory of accommodation [1]. Researches into understanding accommodation and restoring accommodative function of the eye for millions of people with presbyopia and cataract surgery have attracted great interest among the ophthalmic research community [2–7].

A quantitative high resolution imaging technique that can image the whole anterior segment (the cornea, iris, and crystalline lens) in real time is highly desired and will greatly benefit the research in accommodation. However, currently there is no *in vivo* imaging technology that can meet all the needs for measuring the modifications of the anterior segment during accommodation, which we believe is one of the major hurdles for the research on accommodation and reasons why the arguments about the mechanisms are still surprisingly vehement [2–7]. The conventional technologies for anterior segment imaging are Scheimpflug photography, A / B scan ultrasound, UBM (Ultrasound Biomicroscopy), slit scanning topography, and Purkinje imaging [5,8–13]. With these technologies, it is necessary to stimulate the fellow eye in order to observe the variations of the analyzed eye. The techniques

**E-mail: sjiao@usc.edu.
[3]Current address: Department of Ophthalmology, Keck School of Medicine, University of Southern California, 1450 San Pablo, Los Angeles, CA 90033, USA
*Authors have the same contribution to the project

OCIS codes: (170.4500) Optical coherence tomography; (330.5370) Physiological optics; (170.4580) Optical diagnostics for medicine

using ultrasound can only be used with contact systems or with water baths that will modify the anatomical dimensions or the pressure of the anterior segment. Geometrical reconstructions are necessary with the Scheimpflug photographic technique while it cannot be used in certain axes. The eye also needs to be dilated for Scheimpflug photography, which is not a natural condition for accommodation. MRI (magnetic resonance imaging) was also used to image the anterior segment of the eye by some authors [12]. But it may not be routinely used.

Optical coherence tomography (OCT) is a low-coherence interferometer-based noninvasive medical imaging modality that can provide high-resolution cross sectional images of biological tissues [14,15]. Anterior segment OCT (AS-OCT) provides the advantage of producing non-contact images of the anterior segment in static and dynamic conditions [16–34]. AS-OCT was first reported by Izatt *et al.* using a time-domain system with a superluminescent diode light source at 800 nm [16]. Baikoff *et al.* [32,33] and Richdale *et al.* [34] explored the modifications of the anterior chamber and lens thickness with aging and accommodation using time-domain AS-OCT. However, simultaneous imaging of the whole anterior segment (cornea, iris, anterior chamber and crystalline lens) cannot be realized with commercial time-domain AS-OCT system because of the limitation of imaging depth as well as imaging speed. Because all the surfaces of the anterior segment cannot be imaged simultaneously, the contribution of the posterior surface curvature of the lens to accommodation, which may also play a significant role, was not discovered in their studies. Furthermore, when imaging the posterior surface of the lens with conventional AS-OCT usually only one specular reflection spot appears in the image, which makes it impossible to calculate the curvature of the surface. The accuracy of the measurement of the lens thickness is also not reliable when only one spot on the posterior surface can be detected.

The application of spectral domain OCT (SD-OCT) in imaging the anterior segment of the eye has been reported by several groups [17–28]. SD-OCT provided unprecedented imaging speed, and thus made possible 3D imaging of the anterior segment of the eye. However, the limited imaging depth in SD-OCT also made imaging the whole anterior segment formidable. To improve the imaging depth in SD-OCT several groups have developed techniques to eliminate the mirror image [19–22,27]. The most recent development by Grulkowski *et al.* [22] represents a big step toward real time imaging of the whole anterior segment of the eye using a high-speed CMOS camera. However, if only single OCT channel is used, these techniques reduce the imaging speed the same system can achieve since multiple images need to be acquired to remove the complex ambiguity in SD-OCT. Another limitation in imaging the whole anterior segment is the limited depth of focus of the objective lens. Unless dynamic focusing is employed, which is not suitable for high speed imaging, the depth of focus cannot cover the depth of the whole anterior segment. Multiple-channel [23,26] and multiple-focus OCT [35–37] offer possible solutions to the problem.

In the present work, we developed a dual channel dual focus SD-OCT system to image all the surfaces of the anterior segment of the eye simultaneously for studying accommodation of the eye. This technique provides a powerful imaging tool for research on the mechanism of accommodation and presbyopia.

2. Experimental system and performance

A schematic of the experimental system is shown in Fig. 1. The OCT system consisted of two fiber-based Michelson interferometers with two independent spectrometers for detecting the combined light from the reference and sample arms. The scanning and optical delivery system was built on a modified slit lamp with a video camera for guiding the imaging operation. The sample light beams coming out of the sample fibers were combined by a beam-splitter cube and then scanned and delivered to the eye by the same x–y galvanometer scanner and optics.

The two probing beams were coaxial but focused at different depth in the eye: The light beam responsible for imaging the cornea and the anterior surface of the lens (OCT-1, consisting of light source SLD1, optics of channnel1, and spectrometer 1) was focused at the anterior chamber while the other light beam (OCT-2, consisting of light source SLD2, optics of channel 2, and spectrometer 2) was focused at the posterior surface of the lens. The spectrometer in OCT-1 was specifically designed for the study, which has a calibrated imaging depth of 5.2 mm in air. The spectrometer in OCT-2 is borrowed from our previously built machine for high resolution retinal imaging, which has a calibrated imaging depth of 2.5 mm. Two superluminescent diode-based light sources (SLD, Inphenix, USA and Superlum, Russia) with FWHM bandwidths of 50nm and 100nm were used for the two OCT systems, respectively. With the same center wavelength of 840 nm the calibrated depth resolutions are 6μm and 3.3μm in air for OCT-1 and OCT-2, respectively. The linear CCD cameras (Aviiva-SM2-CL-2014, 2048 pixels with 14 micron pixel size operating in 12-bit mode, e2V) in the two spectrometers were synchronized and operating at a rate of 24k lines per second.

To tune the system we first adjust the reference arm of OCT-1 so the cornea and the anterior chamber can be imaged with the reference plane being placed in front of the cornea. We then adjust the reference arm of OCT-2 so the back surface of the lens can be imaged. The distance between the two OCT images was then measured with a mirror as a sample, which was mounted on a translation stage in the sample arm. The measured distance was 3.325 mm in air. Knowing the distance between the images a composite cross-sectional image can be constructed from them. Then all the surfaces of the anterior segment can be imaged simultaneously with the two OCT subsystems. The optimizing process is as following: (1) the objective lens was adjusted to optimize the images of OCT-1; (2) the collimating lens for OCT-2 was adjusted to optimize the image of the back surface of the lens.

The optical path length difference between the two reference arms was 11.025mm, which is the addition of the imaging depths in air of OCT-1 and OCT-2 and 3.325mm. Since the distance between the two reference arms is bigger than the sum of the imaging depths of the two OCT systems, there's a gap between the two simultaneous OCT images. As a result, the core of the lens was not imaged. However, this has no effect in the study of accommodation.

The two OCT subsystems have a similar sensitivity of 95dB and a 20dB sensitivity drop at the maximal imaging depth. The lateral resolution and the depth-of-focus are 20μm and 3.7mm, respectively. The total exposure power at the surface of the cornea was 1.4mW, which is safe for long exposure to the eye according to ANSI Z136.1 (The light was focused on the anterior segment not the retina). The fast image acquisition speed (24k lines per second) is potentially suitable for dynamic and real time imaging of accommodation and helpful for reduction of motion error.

The optical distance of a target to the eye was changed with the movement of the target or lens L2, therefore the amplitude of accommodation can be controlled subjectively assuming that the subject could see the target as clearly as possible. Both the OCT channels are controlled by a single computer and the whole anterior segment of the eye is imaged simultaneously in real time.

3. Results and discussions

3.1 Simultaneous imaging of the anterior segment of the eye

The right eye of one of the authors (37-year old, −3.50D) was imaged. During the imaging, the same eye was fixated on a letter chart (Fixating target as shown in Fig. 1) which is movable along the optical axis in the experimental setup. The volunteer was asked to see a letter as clearly as possible when the image was acquired in real time. So the amplitude of

accommodation can be determined subjectively with the optical distance of the letter chart to the cornea. The eye was imaged in relaxed status then imaged immediately with 2.00D subjective accommodation in test session 1 and 5.50D subjective accommodation in test session 2, respectively. The interval between two test sessions was about 15 minutes.

The simultaneous acquisition of the two raw images using the dual channel dual focus OCT is shown in Fig. 2. The cross-sections (B-Scans) consisting of 2048 A-scans are shown in Fig. 2 (a) and (b). The imaging ranges in Fig. 2 (a) an (b) are 5.2mm and 2.5mm in air, respectively. The images are then constructed in scale according to the method described in section 2 (Fig. 3). The whole anterior segment of the eye, including cornea, anterior chamber angle, iris, anterior and posterior surfaces of the capsule and lens, is clearly visualized.

The constructed images are optically corrected for image warping with the corneal refractive index of 1.389 for 820nm light using a home-developed software (Fig. 4). The algorithm for the correction is based on the paper by V. Westphal, *et al.* [38]. The distortion to the OCT images is mainly caused by the curved boundary between the cornea and air. The difference of refractive index among the aqueous humour, lens, and vitreous body is relatively small, which cause negligible distortion of the OCT images.

The change of the shape of the iris can also be observed in the acquired images. In accommodation status the iris becomes flattened with fewer folds, and the peripheral anterior chamber becomes more spacious with the contraction of the iris sphincter muscle.

We should admit that the current system was not operating in an optimized condition. We can see that except the apex the upper part of the cornea isn't as visible as the posterior part of the anterior chamber in the OCT-1 images. We believe the reason for the unsatisfactory image quality is the position of the focal plane. The whole lens was not imaged in the current study because the imaging depth of one of the subsystems (OCT-2) is only 2.5mm. This problem can be solved by replacing OCT-2 with a system the same as OCT-1, which has an imaging depth of 5.2mm.

3.2 Modifications of the anterior segment of the accommodated eye

The dimensions of the anterior segment of the eye, including the central thickness of cornea and lens, horizontal radii of curvature of the anterior and posterior surface of the lens, were calculated based on the acquired images. To determine the radius of curvature the boundary was first segmented manually. The data were then fitted with a circle. The changes of the dimensions were also calculated in relaxed and accommodated status (Table 1).

Central corneal thickness didn't change with the test sessions and with the accommodated status of the eye. The lens became thicker in the accommodated eye than in relaxed eye. And the depth of the anterior chamber (measured from the apex of cornea to anterior surface of lens) increased with accommodation. Table 1 also shows the increase of the lens curvature at both anterior and posterior surfaces of the lens. The accommodation amplitude was calculated from the distance between the fixating target and the eye.

The differences between the dimensions measured in the condition without accommodation (columns 1 and 4 of Table 1) are relatively high except that of the central corneal thickness. Since accommodation has little influence on CCT, we guess that the poor repeatability of the measurements of other parameters in the relaxed status may be caused by the following factors: 1). The subject might not be completely relaxed in the tests for the condition without accommodation: the different residual accommodation status might result in different baselines in these two test sessions. 2). The possible alignment error between the test sessions. These

two factors also exist in accommodation research using other methods, the effect of which should be minimized though systematic experimental design.

4. Conclusions

In conclusion, we developed a dual channel dual focus OCT system for real-time imaging of the accommodation of the eye. This experimental system provides simultaneous imaging of the whole anterior segment. Thus the modification of the dimensions of the anterior segment, more particularly the curvatures of the anterior and posterior surface of the lens with accommodation can be studied non-invasively using high resolution OCT. The preliminary results presented in this paper demonstrated the feasibility of this approach. However, some technical details should be optimized and improved in our future work.

The merits of the technique can be summarized as follows:

- **i.** Since two independent channels are used in the system, the imaging speed can be as fast as the CCD camera can reach.
- **ii.** Since two channels are used the focal planes of the two channels can be in different depth and can be adjusted independently in the tissue so that the regions of interest can be selectively enhanced.

The weakness of the current system can be summarized as follows:

- **i.** Since two OCT subsystems are needed the cost for the system is higher
- **ii.** The whole lens was not imaged with our current system because the imaging depth of one of the subsystems (OCT-2) is only 2.5mm. However, this problem can be solved by replacing OCT-2 with a system the same as OCT-1, which has an imaging depth of 5.2mm
- **iii.** Since a beamsplitter was used to couple the two OCT channels, the reflected light in the sample arm was attenuated 50% for each channel, which affects the signal-to-noise ratio of the system. However, this problem can be solved if we use two light sources at different bands, for example one at 840 nm and one at 1050 nm, and a dichroic mirror is used to couple the two channels

Acknowledgment

The research was supported in part by NIH grant 1R21 EB008800-01 and “111” project from Ministry of Education, China [No. B08020].

References and links

1. Helmholtz H. Ueber die Accommodation des Auges. Albrecht von Graefes Arch Ophthalmo 1855;2 (1):1–74.
2. Schachar RA. Is Helmholtz’s theory of accommodation correct? Ann. Ophthalmol 1999;31:10–17.
3. Coleman DJ. Unified model for accommodative mechanism. Am. J. Ophthalmol 1970;69(6):1063–1079. [PubMed: 5423772]
4. Glasser A, Kaufman PL. The mechanism of accommodation in primates. Ophthalmology 1999;106 (5):863–872. [PubMed: 10328382]
5. Koretz JF, Cook CA, Kaufman PL. Accommodation and presbyopia in the human eye. Invest. Ophthalmol. Vis. Sci 1997;38(3):569–578. [PubMed: 9071209]
6. Atchison DA. Accommodation and presbyopia. Ophthalmic Physiol. Opt 1995;15(4):255–272. [PubMed: 7667018]
7. Charman WN. The eye in focus: accommodation and presbyopia. Clin. Exp. Optom 2008;91(3):207–225. [PubMed: 18336584]

8. Wolffsohn JS, Davies LN. Advances in anterior segment imaging. Curr. Opin. Ophthalmol 2007;18 (1):32–38. [PubMed: 17159445]
9. Kirschkamp T, Dunne M, Barry JC. Phakometric measurement of ocular surface radii of curvature, axial separations and alignment in relaxed and accommodated human eyes. Ophthalmic Physiol. Opt 2004;24(2):65–73. [PubMed: 15005670]
10. Vilupuru AS, Glasser A. Dynamic accommodative changes in rhesus monkey eyes assessed with A-scan ultrasound biometry. Optom. Vis. Sci 2003;80(5):383–394. [PubMed: 12771664]
11. Ishikawa H, Schuman JS. Anterior segment imaging: ultrasound biomicroscopy. Ophthalmol. Clin. North Am 2004;17(1):7–20. [PubMed: 15102510]
12. Koretz JF, Strenk SA, Strenk LM, Semmlow JL. Scheimpflug and high-resolution magnetic resonance imaging of the anterior segment: a comparative study. J. Opt. Soc. Am. A 2004;21(3):346–354.
13. Rosales P, Dubbelman M, Marcos S, van der Heijde R. Crystalline lens radii of curvature from Purkinje and Scheimpflug imaging. J. Vis 2006;6(10):1057–1067. [PubMed: 17132077]
14. Huang D, Swanson EA, Lin CP, Schuman JS, Stinson WG, Chang W, Hee MR, Flotte T, Gregory K, Puliafito CA, Fujimoto JG. Optical coherence tomography. Science 1991;254(5035):1178–1181. [PubMed: 1957169]
15. Fercher AF. Optical coherence tomography. J. Biomed. Opt 1996;1(2):157–173.
16. Izatt JA, Hee MR, Swanson EA, Lin CP, Huang D, Schuman JS, Puliafito CA, Fujimoto JG. Micrometer-scale resolution imaging of the anterior eye in vivo with optical coherence tomography. Arch. Ophthalmol 1994;112(12):1584–1589. [PubMed: 7993214]
17. Kaluzny JJ, Wojtkowski M, Kowalczyk A. Imaging of the anterior segment of the eye by Spectra Optical Coherence Tomography. Optica Applicata 2002;32:581–589.
18. Kaluzny BJ, Kaluzy BJ, Kałuzny JJ, Szkulmowska A, Gorczyńska I, Szkulmowski M, Bajraszewski T, Wojtkowski M, Targowski P. Spectral optical coherence tomography: a novel technique for cornea imaging. Cornea 2006;25(8):960–965. [PubMed: 17102675]
19. Baumann B, Pircher M, Götzinger E, Hitzenberger CK. Full range complex spectral domain optical coherence tomography without additional phase shifters. Opt. Express 2007;15(20):13375–13387. [PubMed: 19550607]
20. Targowski P, Gorczynska I, Szkulmowski M, Wojtkowski M, Kowalczyk A. Improved complex spectral domain OCT for in vivo eye imaging. Opt. Commun 2005;249(1–3):357–362.
21. Sarunic MV, Asrani S, Izatt JA. Imaging the ocular anterior segment with real-time, full-range Fourier-domain optical coherence tomography. Arch. Ophthalmol 2008;126(4):537–542. [PubMed: 18413525]
22. Grulkowski I, Gora M, Szkulmowski M, Gorczynska I, Szlag D, Marcos S, Kowalczyk A, Wojtkowski M. Anterior segment imaging with Spectral OCT system using a high-speed CMOS camera. Opt. Express 2009;17(6):4842–4858. [PubMed: 19293916]
23. Gotzinger E, Pircher M, Leitgeb RA, Baumann B, Hitzenberger CK. Quadruple depth range spectral domain optical coherence tomography for imaging of the anterior eye segment. presented at the SPIE Photonics West on Bios, San Jose, CA, USA 2009 Jan;:24–29.
24. Yasuno Y, Madjarova VD, Makita S, Akiba M, Morosawa A, Chong C, Sakai T, Chan KP, Itoh M, Yatagai T. Three-dimensional and high-speed swept-source optical coherence tomography for in vivo investigation of human anterior eye segments. Opt. Express 2005;13(26):10652–10664. [PubMed: 19503280]
25. Kerbage C, Lim H, Sun W, Mujat M, de Boer JF. Large depth-high resolution full 3D imaging of the anterior segments of the eye using high speed optical frequency domain imaging. Opt. Express 2007;15(12):7117–7125. [PubMed: 19547029]
26. Grajciar B, Pircher M, Hitzenberger CK, Findl O, Fercher AF. High sensitive measurement of the human axial eye length in vivo with Fourier domain low coherence interferometry. Opt. Express 2008;16(4):2405–2414. [PubMed: 18542319]
27. Targowski P, Wojtkowski M, Kowalczyk A, Bajraszewski T, Szkulmowski M, Gorczyńska I. Complex spectral OCT in human eye imaging in vivo. Opt. Commun 2004;229(1–6):79–84.
28. Götzinger E, Pircher M, Leitgeb RA, Hitzenberger CK. High speed full range complex spectral domain optical coherence tomography. Opt. Express 2005;13:583–594. [PubMed: 19488388]

29. Konstantopoulos A, Hossain P, Anderson DF. Recent advances in ophthalmic anterior segment imaging: a new era for ophthalmic diagnosis? Br. J. Ophthalmol 2007;91(4):551–557. [PubMed: 17372341]

30. Nolan W. Anterior segment imaging: ultrasound biomicroscopy and anterior segment optical coherence tomography. Curr. Opin. Ophthalmol 2008;19(2):115–121. [PubMed: 18301284]

31. Goldsmith JA, Li Y, Chalita MR, Westphal V, Patil CA, Rollins AM, Izatt JA, Huang D. Anterior chamber width measurement by high-speed optical coherence tomography. Ophthalmology 2005;112(2):238–244. [PubMed: 15691557]

32. Baikoff G, Lutun E, Wei J, Ferraz C. Anterior chamber optical coherence tomography study of human natural accommodation in a 19-year-old albino. J. Cataract Refract. Surg 2004;30(3):696–701. [PubMed: 15050270]

33. Baikoff G, Lutun E, Ferraz C, Wei J. Static and dynamic analysis of the anterior segment with optical coherence tomography. J. Cataract Refract. Surg 2004;30(9):1843–1850. [PubMed: 15342045]

34. Richdale K, Bullimore MA, Zadnik K. Lens thickness with age and accommodation by optical coherence tomography. Ophthalmic Physiol. Opt 2008;28(5):441–447. [PubMed: 18761481]

35. Holmes J, Hattersley S, Stone N, Bazant-Hegemark F, Barr H. Multi-channel Fourier domain OCT system with superior lateral resolution for biomedical applications. Proc. SPIE 6847 2008:68470O.

36. Holmes J. Theory and applications of multi-beam OCT. Proc. SPIE 7139 2008:713908.

37. Holmes J, Hattersley S. Image blending and speckle noise reduction in multi-beam OCT. Proc. SPIE 7168 2009:71681N.

38. Westphal V, Rollins AM, Radhakrishnan S, Izatt JA. Correction of geometrical and refractive image distortions in optical coherence tomography applying Fermat's principle. Opt. Express 2002;10:397–403. [PubMed: 19436373]

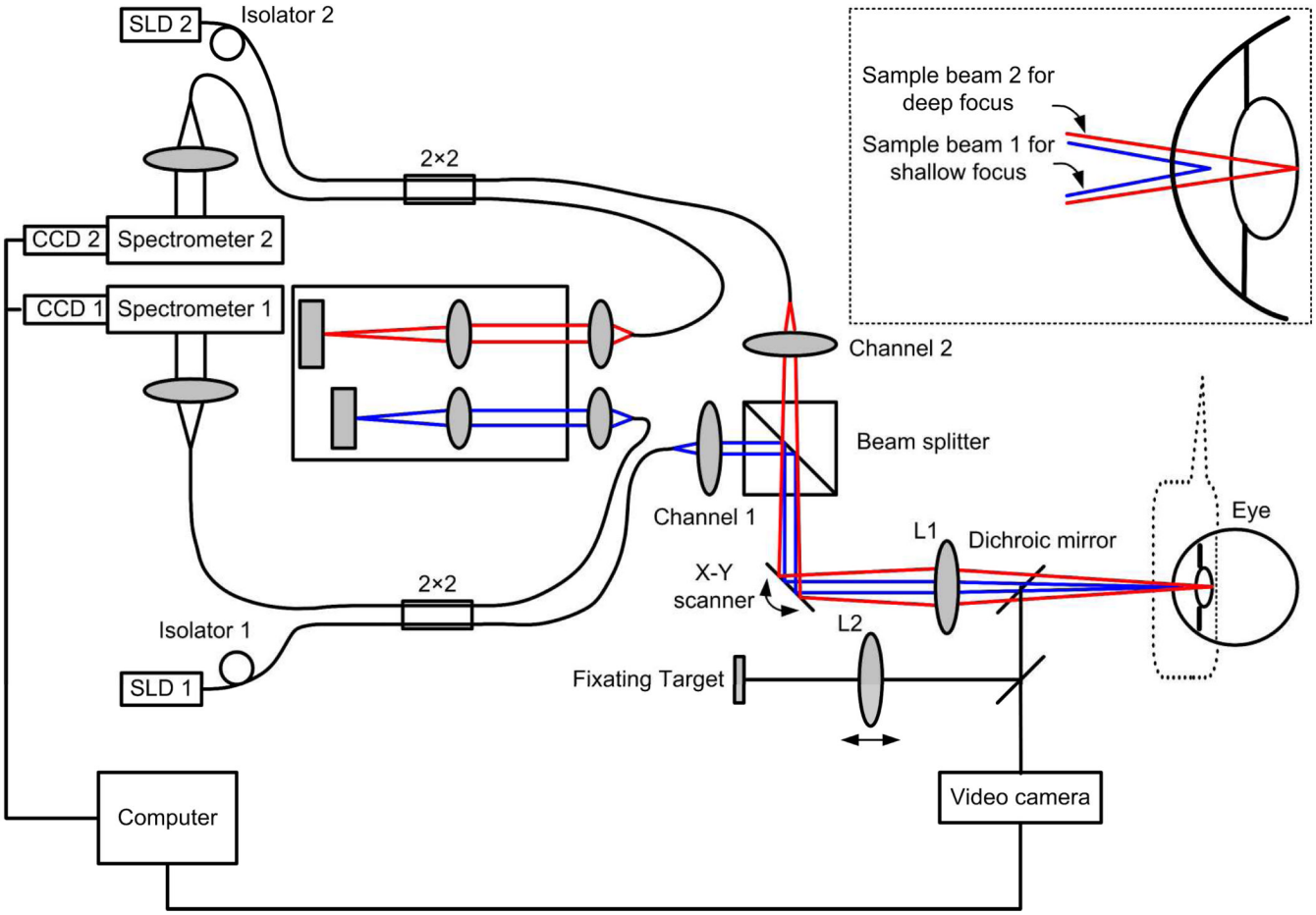

Fig. 1.

Schematic of the dual channel OCT experimental system. The inserted is the enlargement of the dual focus configuration of two sample beams.

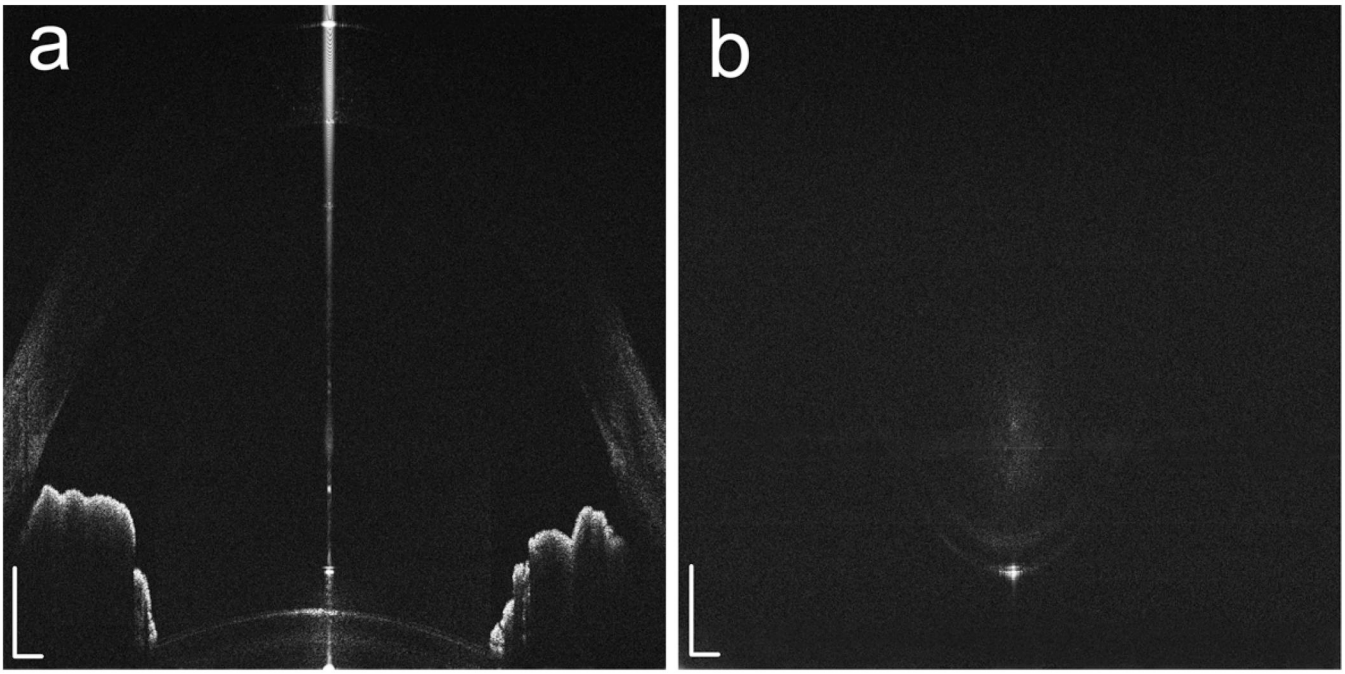

Fig. 2.
The simultaneously acquired raw images using the dual channel dual focus OCT show the anterior chamber (a) and the posterior surface of the lens (b), respectively. These two images have a distance of 3.325mm in air in the depth direction. Pixels: 2048 × 2048; Imaging range: 5.2 (depth) × 12 (width) mm (a) and 2.5 (depth) × 12 (width) mm (b); White bar: 0.5mm.

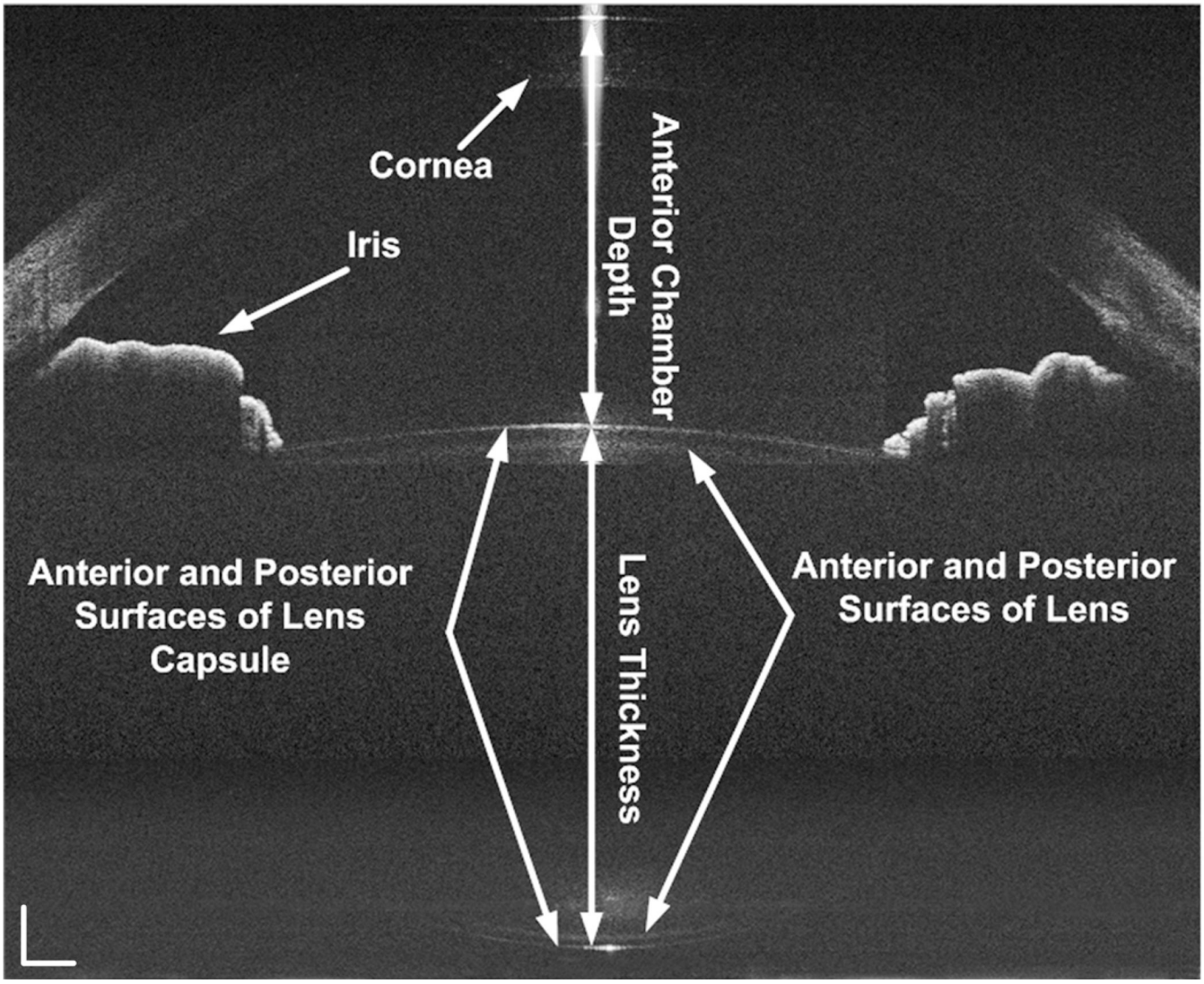

Fig. 3.

The simultaneously acquired images were constructed in scale, but with optical correction. All the surfaces of the anterior segment of the eye including the cornea, anterior chamber, anterior and posterior surfaces of crystalline lens and capsule were clearly visualized. The white bar: 0.5mm.

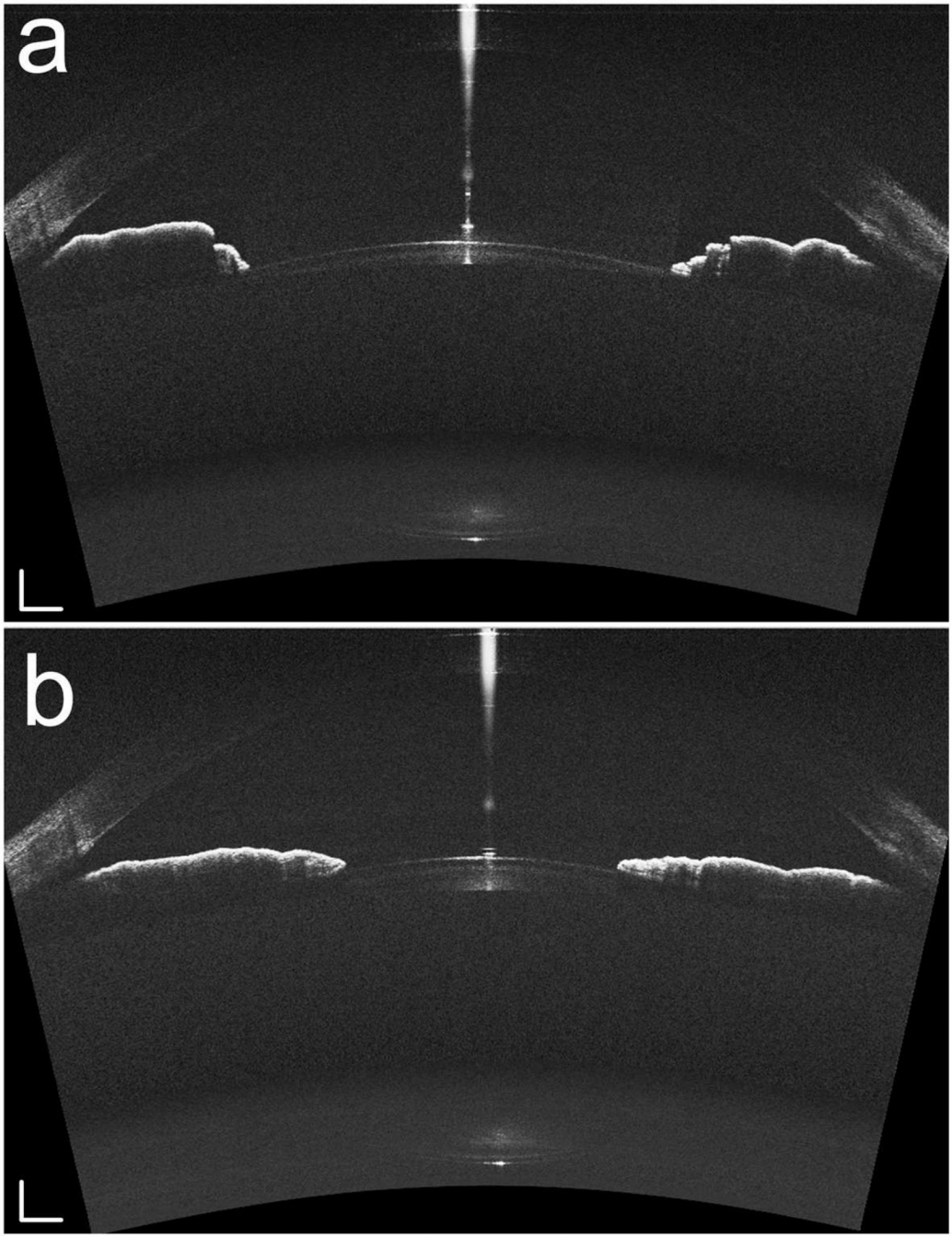

Fig. 4.
The right eye (−3.50D myopic) of the subject was imaged without accommodation (a) and with 5.5 D accommodation (b). The white bar: 0.5mm.

Table 1

Dimensions of the anterior segment in relaxed and accommodated eye. The accommodation amplitude is 2.00D in test session 1 and 5.50D in test session 2, respectively.

	Session1: 2.00D ACC			*Session 2: 5.50D ACC*		
	Without ACC	**With ACC**	**Delta**	**Without ACC**	**With ACC**	**Delta**
CCT	0.550	0.552	0.002	0.550	0.550	0
ACD	3.342	3.325	−0.017	3.420	3.287	−0.133
RAL	9.614	8.299	−1.315	10.511	9.797	−0.714
RPL	6.171	5.444	−0.727	5.761	4.802	−0.959
LT	4.037	4.083	0.046	4.160	4.284	0.124

ACC = Accommodation, CCT = Central cornea thickness, ACD = Anterior chamber depth, RAL = Horizontal radius of curvatures of the anterior lens surface, RPL = Horizontal radius of curvatures of the posterior lens surface, LT = Lens thickness, Delta = the differences of the value between accommodation (With ACC) and without accommodation (Without ACC). All units in the table are mm.